A digital, constant-frequency pulsed phase-locked-loop instrument for real-time, absolute ultrasonic phase measurements

H. A. Haldren,[1,a),b)] D. F. Perey,[2] W. T. Yost,[2] K. E. Cramer,[2] and M. C. Gupta[1]
[1]*Charles L. Brown Department of Electrical and Computer Engineering, University of Virginia, Thornton Hall, 351 McCormick Rd., Charlottesville, Virginia 22904, USA*
[2]*Nondestructive Evaluation Sciences Branch, NASA Langley Research Center, 4 Langley Blvd., Building 1230, MS 231, Hampton, Virginia 23681, USA*

(Received 19 January 2018; accepted 18 April 2018; published online 8 May 2018)

A digitally controlled instrument for conducting single-frequency and swept-frequency ultrasonic phase measurements has been developed based on a constant-frequency pulsed phase-locked-loop (CFPPLL) design. This instrument uses a pair of direct digital synthesizers to generate an ultrasonically transceived tone-burst and an internal reference wave for phase comparison. Real-time, constant-frequency phase tracking in an interrogated specimen is possible with a resolution of 0.000 38 rad (0.022°), and swept-frequency phase measurements can be obtained. Using phase measurements, an absolute thickness in borosilicate glass is presented to show the instrument's efficacy, and these results are compared to conventional ultrasonic pulse-echo time-of-flight (ToF) measurements. The newly developed instrument predicted the thickness with a mean error of −0.04 μm and a standard deviation of error of 1.35 μm. Additionally, the CFPPLL instrument shows a lower measured phase error in the absence of changing temperature and couplant thickness than high-resolution cross-correlation ToF measurements at a similar signal-to-noise ratio. By showing higher accuracy and precision than conventional pulse-echo ToF measurements and lower phase errors than cross-correlation ToF measurements, the new digitally controlled CFPPLL instrument provides high-resolution absolute ultrasonic velocity or path-length measurements in solids or liquids, as well as tracking of material property changes with high sensitivity. The ability to obtain absolute phase measurements allows for many new applications than possible with previous ultrasonic pulsed phase-locked loop instruments. In addition to improved resolution, swept-frequency phase measurements add useful capability in measuring properties of layered structures, such as bonded joints, or materials which exhibit non-linear frequency-dependent behavior, such as dispersive media. *Published by AIP Publishing.* https://doi.org/10.1063/1.5022989

I. INTRODUCTION

Ultrasonic phase measurements have been used for many years to measure absolute and relative material properties. The phase, rather than the amplitude, of ultrasonic waves is ideally suited for these measurements due to its sensitivity to the wavelength and thickness of a material specimen. Methods of accurately determining the time delay between received ultrasonic echoes date back as far as the 1960s with the pulse-superposition method by McSkimin[1] and the pulse-echo-overlap method by Papadakis.[2] Several improvements to broadband time-domain ultrasonic velocity-change measurements with damped transducers have been made throughout the years.[3–6] Other pulse-echo methods involve finding the resonance frequency of the material[7,8] or utilize continuous-wave sources to introduce standing waves rather than broadband sources.[9] A comprehensive overview of high-resolution ultrasonic velocity measurement methods in liquids was compiled by Kaatze, Eggers, and Lautscham.[10]

Another method of measuring ultrasonic time delays focuses on the cross correlation between transmitted and received ultrasonic pulses, where the peak of the cross-correlation function indicates the time-of-flight (ToF) of the ultrasonic signal within the specimen.[11] Cross-correlation ToF measurements can be setup entirely digitally to monitor ultrasonic propagation changes within a system, and it is well suited for cases where the signal amplitude may vary significantly due to attenuation and scattering. The cross-correlation method has been applied to cases of ultrasonic velocity measurements,[12–15] flow monitoring,[16] distance measurements,[17] and material crack and flaw identification.[18] Liang *et al.* investigated the fundamental limits of cross-correlation-based phase measurements, describing phase errors introduced by quantization as well as non-integral sampling.[19] While improving ToF accuracy and precision over conventional methods, cross correlation suffers from the time and computational expense needed for post-processing of the transmitted and received signals to find the ToF, limiting its ability to provide inexpensive real-time ToF monitoring for certain applications.

For high-accuracy measurements, single frequency gated continuous wave (tone-burst) ultrasonic techniques increase the signal-to-noise ratio of their broadband counterparts. By comparing a received ultrasonic wave signal with a reference signal and adjusting the driving frequency until the waves are in quadrature ($\pi/2$ phase difference), a highly

a)Author to whom correspondence should be addressed: hah5bc@virginia.edu
b)This research was performed while H. Haldren was at NASA Langley Research Center, Hampton, Virginia 23681, USA.

sensitive measurement of changes in sound velocity or material thickness is obtained.[20] The phase comparison technique has since spawned several variations of pulsed phase-locked loop (PPLL) ultrasonic phase measurement methods.

The initial variable-frequency PPLL systems were used in applications of bolt tension monitoring,[21] as well as detecting changes in sound velocity.[22] A major drawback of variable-frequency phase measurement methods is their sensitivity to frequency-dependent sources of phase error in the instrumentation electronics, transducers, and material. Furthermore, variable-frequency methods are unable to measure true phase changes within a specimen, as they rely on changing frequency to make a single-phase measurement. Consequently, the constant-frequency PPLL (CFPPLL) provides a major improvement for conducting ultrasonic phase measurements.[22]

The original CFPPLL design utilized a single driving frequency, a voltage-controlled phase shifter, and a phase detector to lock the transmitted and reference waves in quadrature.[23] This instrument measured absolute phase velocities in liquids by tracking the phase shift induced when changing the ultrasonic path length; however, only changes in ultrasonic velocity due to external stimuli, such as pressure or temperature, were measurable in solids. Nonetheless, in comparison to the variable frequency PPLL counterpart, the CFPPLL provided very high accuracy and sensitivity.

A digitally controlled CFPPLL instrument capable of real-time ultrasonic tracking of phase and swept-frequency phase measurements on both solids and liquids is explored. This instrument offers significant improvements in ease-of-use due to digital control and data collection capabilities. Whereas previous PPLL-based instruments required the changing of the path-length to conduct absolute sound velocity measurements in liquids, both constant-frequency phase tracking and phase vs. frequency measurements of this CFPPLL instrument permit other experimental approaches. To illustrate this flexibility, experimental measurements of small differences in path-length in borosilicate glass via the CFPPLL instrument are shown and compared with conventional pulse-echo time-of-flight (ToF) measurements for thickness measurement accuracy and precision.

To obtain high accuracy phase measurements, the internal and external sources of uncertainty with this method were examined in detail. While simple pulse-echo ToF measurements are often sufficient for ultrasonic velocity measurements for flaw detection in large industrial parts, high accuracy phase measurements are extremely important in the measurement of ultrasonic velocity for other disciplines, including the aerospace, automotive, material science, and medical industries. In particular, high-resolution ultrasonic velocity measurements have been used to measure clamping force in bolts under high tension,[24] gas and liquid flow metering,[16] phase diagrams of superconductors,[25] grain size estimation in steel,[26] human bone quality,[27] and molecular relaxation processes.[28] Additionally, high-resolution ultrasonic phase measurements have proved able to noninvasively measure intracranial pressure, which has classically only been measurable invasively.[29] Without corrections for commonly encountered external factors, such as transducer coupling and temperature variations, the accuracy of these highly sensitive techniques is greatly affected.

II. THE DIGITALLY CONTROLLED CONSTANT FREQUENCY PULSED PHASE-LOCKED LOOP

All PPLL devices consist of two signal paths along which the first, an ultrasonically transceived tone-burst, is phase-compared to a reference wave. On Path 1, the transducer generates an ultrasonic tone-burst which traverses a material specimen. In a pulse-echo arrangement, the same transducer receives and converts the tone-burst back into an electrical signal, while in a pitch-catch arrangement, a second transducer is used to receive the tone-burst. On Path 2, the reference wave is phase-compared to the transceived tone-burst from the first path. In a variable-frequency PPLL, the frequency of the transceived tone-burst is varied until the signals are in quadrature, while in a CFPPLL, the relative phase of the transceived signal is changed. The system is then considered to be in a locked state, and quadrature is maintained through continual updates to frequency or relative phase of the transceived signal.

In the digitally controlled CFPPLL instrument, a pair of direct digital synthesizers (DDSs) generates sine waves with a repeatable constant phase offset, permitting absolute ultrasonic phase measurements. While the system is in a locked state, the voltage output of a phase-detector is sampled by a microcontroller, which commands the DDS to adjust the transceived tone-burst's phase to maintain the quadrature with the reference wave. A field-programmable gate array (FPGA) controls timing parameters and gating within the system.

A block diagram of the developed CFPPLL-based ultrasonic phase measurement instrument is shown in Fig. 1. Using a computer terminal, the user adjusts waveform and system parameters such as the sample-and-hold (S/H) position, number of tone-burst cycles, repetition rate of the tone-burst, and number of sampled data points to average when taking phase measurements. After initial setup, the user locks the system which outputs the phase adjustments to the computer.

The twin DDSs generate sine waves at the frequency, amplitude, and phase set by the microcontroller. The same 1 GHz input timing clock is used for both DDSs, and upon system startup, the microcontroller synchronizes their output via a simultaneous reset command. The DDSs use lookup tables to generate the frequency and phase of the ultrasonic waves, which provide absolute frequency and phase adjustment resolution limits. The DDSs have 14 bits of phase resolution and 48 bits of frequency resolution, resulting in a minimum phase shift of $2\pi/2^{14} \approx 0.000\,38$ (rad) $\approx 0.022°$ and a minimum frequency shift of ~3.55 μHz. Based on the timing information set by the microcontroller, the FPGA uses a transmit enable (TX EN) signal to gate the transceived wave in Path 1, forming a tone-burst of a set number of cycles.

Unlike other time-delay measurement methods, the phase resolution and phase quantization error of the CFPPLL method is not frequency dependent. Set by the constant phase shift

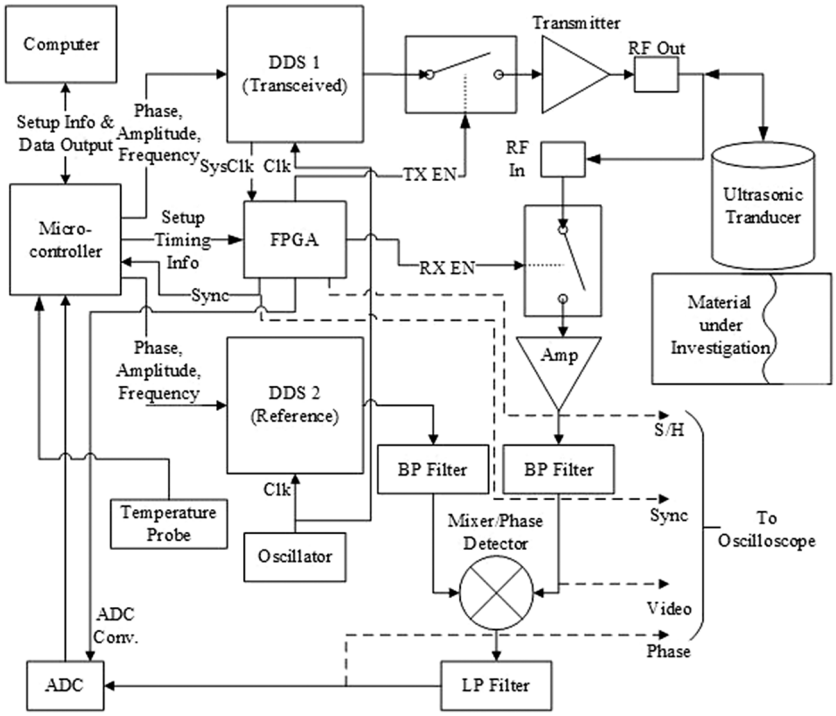

FIG. 1. Block diagram of digitally controlled CFPPLL instrument.

resolution by the DDSs, no matter which frequency of sine waves being generated, the relative phase between the generated sine waves can only be changes in multiples of 0.022°. In contrast to conventional time-delay methods, a consequence of constant phase resolution with this method is that time resolution will be worse for lower frequencies and better for higher frequencies, based on the relationship between time delay and phase, $\Delta t = \Delta\phi/360f$.

The tone-burst in Path 1 is amplified and sent to a transducer, which ultrasonically interrogates a material specimen through a coupling medium. After being reflected off the back wall of the test specimen, the acoustic tone-burst is received by the same transducer in the pulse-echo setup, as shown in Fig. 1. Material property variations due to external stimuli such as pressure, temperature, elasticity, or path length are then detectable via ultrasonic phase shifts. After receiving the ultrasonic reflection, the transducer converts the tone-burst into an electrical signal. The FPGA timing ensures that signals are continuously received using a receive enable (RX EN) signal, except for the short duration during tone-burst transmission.

The received tone-burst is amplified and band-pass filtered to reduce signal noise, and the reference wave passes through an identically designed band-pass filter. Currently, the instrument operates with center frequency around 10 MHz, and the band-pass filtering circuits were both measured to have a −6 dB pass-band of 8.8-11.0 MHz. In practice, commercial damped transducers have displayed wider bandwidths than the band-pass filtering circuits, providing a minimal change to the system bandwidth but providing a measurable phase response which must be characterized for high accuracy phase measurements.

After filtering, the received and reference signals pass into the phase detector. The phase detector outputs a voltage dependent on the phase difference between the two signals, using $\pi/2$ offset at the 0 V reference. The output voltage is low-pass filtered to minimize non-DC noise and is subsequently sampled and held using an analog-to-digital converter (ADC), whose output passes into the microcontroller. The S/H position on the received phase detector output signal is set by the FPGA and is user-specified. Each time the phase output is received by the microcontroller, the voltage output of a temperature probe which is typically adhered to the material test specimen is also sampled.

To properly monitor the system, the SYNC and S/H pulses from the FPGA, the amplitude of the transceived tone-burst after band-pass filtering, and the phase detector output voltage are all viewed on an oscilloscope. Figure 2 shows an example of the oscilloscope CFPPLL signal display. The SYNC signal represents the beginning of each tone-burst transmission and is the trigger for the oscilloscope. The filtered amplitude signal, or video signal in Fig. 1, is used to observe ultrasonic reflections and helps the user determine waveform parameters. Often, the number of transmitted cycles is chosen to minimize the gap between successive reflections without overlapping. The phase and S/H signals are used to set the S/H position, typically in the portion of the received tone-burst where the phase appears flat. It should be noted that there is a slight time delay between the video amplitude signal and the output of the phase detector; thus, the S/H position occurs slightly earlier than it appears on the amplitude signal.

The "bleed-thru" portion of the waveform is never actually transceived ultrasonically but instead stays within the circuit. While the RX EN signal is off during the transmission period, some small amplitude leaks through and is amplified like the received ultrasonic reflections. It was first thought that this "bleed-thru" signal was undesirable; however, it has since

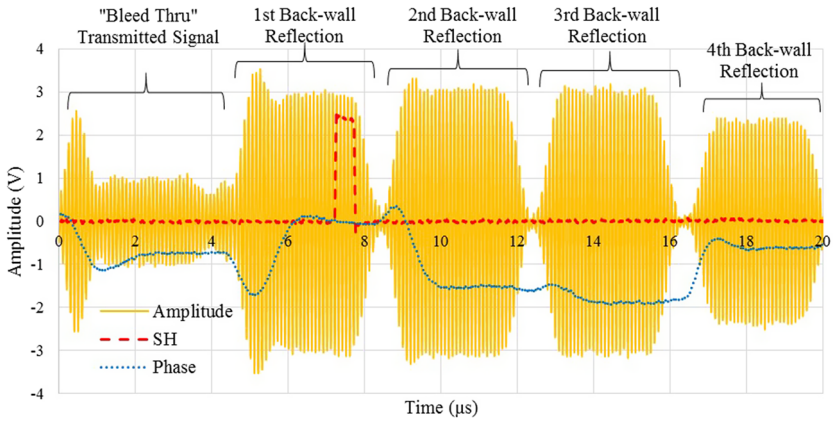

FIG. 2. Typical waveforms of received ultrasonic wave amplitude, phase detector output, and sample and hold (S/H) signals seen on an oscilloscope when using the CFPPLL instrument.

proved useful in measuring the phase response of the filtering circuits.

III. THICKNESS MEASUREMENT IN SOLIDS

A. Method description

Assume that an ultrasonic displacement plane wave is propagating within a non-dispersive medium of finite thickness, Medium 1. After reflection off the boundary with some half-space, Medium 2, and being received, as shown in Fig. 3, the phase of the ultrasonic wave is expressed as

$$\phi_{u_R} = -2k_1L_1 = -720fL_1/c_1 \text{ (deg)}, \quad (1)$$

where $k_1 = \omega/c_1$ is the wavenumber in Medium 1 with sound velocity c_1, $\omega = 2\pi f$ (rad) = $360f$ (deg) is the driving angular frequency with driving frequency f, and L_1 is the thickness of Medium 1. The factor of two occurs due to the propagation through the thickness of Medium 1 twice. It is assumed in Eq. (1) that the acoustic impedance of Medium 1 is greater than that in Medium 2 or else the reflected wave would be π out of phase with the incident wave, as the normal-incidence ultrasonic particle displacement wave reflection coefficient is $R = (Z_1 - Z_2)/(Z_1 + Z_2)$, where Z_j is the acoustic impedance of each medium.

1. Swept-frequency phase measurements

The phase of the reflected wave is used to measure either the sound velocity or thickness of a material, given the other parameter. In non-dispersive media, the group velocity, $c_g = d\omega/dk$, is equal to the phase velocity, $c_p = dx/dt$.[22] Thus, single-frequency phase measurements can find group velocity as well as phase velocity in non-dispersive media.

As the constant-frequency phase measures relative fractions of a wavelength, expressed between $-\pi$ and π, it is difficult to obtain absolute thickness or sound velocity measurements since the total number of propagating wavelengths is unknown. Previous PPLL-based methods could measure absolute sound velocity in fluid media, where the acoustic path length was varied and $\partial\phi_{u_R}/\partial L_1$ was measured.[22,23] In solid media, only changes in sound velocity could be measured as the path length could not be changed.

With the digitally controlled CFPPLL instrument, the ultrasonic driving frequency can be altered while maintaining the phase relationship between the transceived and reference signals, allowing a measurement of $\phi_{u_R}(f)$. By sweeping the driving frequency and measuring the phase response, the sound velocity or specimen thickness is extracted by the relation,

$$\partial\phi_{u_R}/\partial f = -720L_1/c_1 \text{ (deg/Hz)}. \quad (2)$$

2. Pulse-echo time-of-flight measurements

Traditional pulse-echo ultrasound can measure sound velocity or material thickness, given the knowledge of one of the parameters. After sending a broadband ultrasonic pulse through a material, the time-of-flight (ToF) of the received pulse is measured. Given the material setup in Fig. 3, the ToF for reflected waves is found by substituting the relation between the time delay and phase, $\Delta t = \phi/\omega$, into Eq. (1) to find

$$ToF = -2L_1/c_1 \text{ (s)}. \quad (3)$$

As the ToF does not suffer from a limited range of possible values like a constant-frequency phase measurement, a single ToF value can be used to measure the sound velocity or specimen thickness.

3. Reducing other phase shifts/time delays

In a practical direct-contact ultrasonic measurement system, the electronic circuitry, ultrasonic transducer, and ultrasonic couplant layer provide time delays or phase shifts. To avoid these errors, different methods are used to reduce

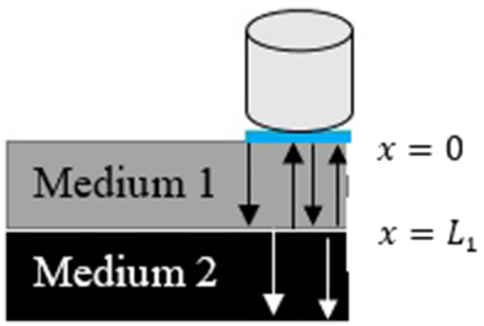

FIG. 3. Representation of ultrasonic wave reflections at the boundary between Medium 1/Medium 2 and the couplant layer.

or negate their effect. In conventional pulse-echo ToF measurements, a primary method for negating external time delays is to measure the ToF difference between successive back-wall echoes from a material. Delays due to the instrumentation, transducer, and double-transmission through the couplant layer affect successive echoes in the same way, so subtracting successive echoes will remove the circuit-based time-delays.

This technique can also be applied to constant-frequency phase measurements. Considering external phase shift sources for ultrasonic echoes from the material system, the measured phase for the nth echo can be described by

$$\phi_n = \phi_{instr.} + \phi_{trans.} + 2\phi_{coup.T} + \phi_D^{(n)} + \phi_{U_R} + (n-1)\left(\phi_{U_R} + \phi_{coup.R}\right), \quad (4)$$

where $\phi_{instr.}$ is the phase shift from the instrumentation, $\phi_{trans.}$ is the phase shift from the ultrasonic transducer, $\phi_{coup.T}$ is the phase shift from transmission through the couplant layer, $\phi_{coup.R}$ is the phase shift from reflection off the couplant layer occurring for secondary echoes, $\phi_D^{(n)}$ is the phase shift due to ultrasonic wave diffraction, and ϕ_{U_R} is the phase shift from the material under investigation as defined in Eq. (1). Note that the superscript on the ϕ_D term corresponds to the diffraction phase shift from the nth echo and is not ϕ_D to the nth power. The phase difference between consecutive reflections from Eq. (4) can be written as

$$\Delta\phi = \phi_{n+1} - \phi_n = \phi_D^{(n+1)} - \phi_D^{(n)} + \phi_{U_R} + \phi_{coup.R}, \quad (5)$$

where several of the external phase shift sources have been eliminated.

Remaining in Eq. (5) is the phase shift of the reflection from the test material-couplant-transducer interface as well as the phase shift due to ultrasonic diffraction. There have been several treatments of the effect of the couplant layer on both the amplitude[30–33] and time-delay[34,35] on an ultrasonic wave. If a bare-element piezoelectric transducer is used, the effect of the couplant layer on the reflected phase can be derived, given the couplant thickness as well as the material properties of the active element, couplant, and material under test.[35] Commercially available broadband ultrasonic transducers, however, contain additional layers which complicate analysis.[34] Furthermore, the internal setup of commercial transducers is often proprietary, which makes the analysis of the ultrasonic reflection coefficient difficult without many assumptions.

Despite difficulties with calculating the actual reflection coefficient from the couplant interface, it can be shown that as the couplant becomes thinner, its effect on the ultrasonic amplitude and phase lessens. By assuming a thin fluid layer between two half-spaces, the effect of a thin couplant layer can be approximated.[36] Assuming a PZT5A transducer, water couplant, and borosilicate glass specimen, the phase of the ultrasonic reflection coefficient as a function of the frequency for different couplant thicknesses is shown in Fig. 4. The difference from the 180° phase shift for an infinitely thin couplant layer becomes more pronounced as the couplant layer thickness becomes larger with respect to the wavelength. As the phase shift can vary dramatically for small differences in thickness, care must be taken

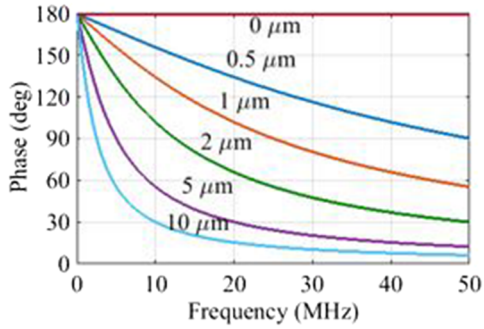

FIG. 4. Phase vs. frequency of ultrasonic reflection off of the couplant interface for different couplant thicknesses.

to ensure a consistent couplant thickness to obtain high repeatability.

The phase of diffraction terms in Eq. (5) can be computed by modeling ultrasonic diffraction within the test specimen for the $(n+1)$th and nth echoes. Due to the use of a finite-radius piston source and receiver, ultrasonic signals do not, in practice, behave as a true plane wave within a specimen. Much research throughout the years has been completed into modeling the effect of diffraction on ultrasonic waves.[37–40] Depending on the unit-less parameter $S = z\lambda/a^2$—where z is the distance traveled, $\lambda = c/f$ is the ultrasonic wavelength, and a is the transducer radius—the amplitude and phase shifts due to diffraction can be calculated. Numerous studies have used corrections for diffraction to obtain more accurate ultrasonic velocity, time-delay, and attenuation measurements.[2,35,41–43] In this work, the exact phase shift due to diffraction due to different back-wall echoes within the test specimen is determined by solving the exact Lommel diffraction correction integral found by Williams[39] and written in a different form by Rogers and Van Buren.[44]

B. Experimental

To demonstrate the capabilities of the CFPPLL-based ultrasonic phase measurement instrument, measurements of micrometer-scale thickness differences in ~11 mm thick smooth glass specimens were performed. Six 5.08 cm × 5.08 cm square specimens were cut from a plate of Schott Borofloat® 33, a float-glass version of borosilicate glass, purchased from S. I. Howard Glass Company. The specimens were cleaned in an ultrasonic bath of ethanol for 30 min prior to testing. Next, a 3 × 3 grid was marked off on each specimen using thin strips of tape to be used for thickness measurements.

At each of the nine locations on the six test specimens, the thickness was measured using a calibrated Starrett micrometer. The micrometer was calibrated by using Starrett-Webber gage blocks in the thickness range of interest, 10.9-11.0 mm, at every 1 μm. After correction, the micrometer measurements in the given range had a standard deviation of error of 1.05 μm.

To maintain a consistent couplant layer thickness between measurements, a screw clamp was used to hold constant pressure and a load cell was placed in the path between the clamp and ultrasonic transducer. An experiment was performed to

vary the pressure on the transducer while measuring the resulting phase shift of reflection from the back-wall of one of the glass specimens.

Another experiment was performed on one of the glass specimens to measure the phase response to temperature change near room temperature. The transducer clamping setup was placed within a custom-built environmental chamber with a temperature stability of ±0.01 °C over 1 h. While holding pressure steady at ~2.8 MPa, the temperature was cycled from 20 °C to 25 °C and the ultrasonic phase response of the first back-wall reflection was monitored at a driving frequency of 10 MHz.

Next, a study was performed on the stability of the constant-frequency ultrasonic phase measurements in the absence of external variables. Again, the transducer clamping setup was placed within the environmental chamber. While holding pressure steady at ~2.8 MPa, the temperature was held constant at 21 °C, and the ultrasonic phase response of the first back-wall echo was monitored at a driving frequency of 10 MHz. While transducer pressure and temperature were held constant, the standard deviation of phase was measured over a 30 min period. To view the effect of averaging, the number of phase measurements averaged when making phase adjustments within the microcontroller was varied from 1 to 256, with a single phase measurement obtained every 6 ms.

Ultrasonic measurements for thickness estimation were taken at each of the nine locations on six test specimens. To maintain a consistent couplant thickness, the transducer was loaded with a pressure of ~2.8 MPa for each test. Water was used as a couplant for all measurements shown in this work due to its well-known material properties; however, other commercially available couplants produced similar results. A 6.35 mm diameter, highly damped, broadband Olympus V112 ultrasonic transducer nominally designed to operate at 10 MHz was used for most measurements, with the exception of some ToF measurements using a 50 MHz transducer.

Using the newly developed CFPPLL-based ultrasonic phase measurement instrument, the phase of the received wave was tracked as the frequency of the input tone-burst varied from 9 MHz to 10 MHz with a 10 kHz resolution. At each frequency, the phase was averaged over 32 repeated tone-bursts to reduce the effect of noise. The phase vs. frequency response of both the first and second back-wall reflections from the Borofloat specimens was measured.

While still under pressure, the ultrasonic transducer was disconnected from the CFPPLL instrument and connected to a GE Panametrics Model 5900PR pulser-receiver to generate and receive broadband pulses for comparative ToF measurements. The generated pulse contained 1 μJ of energy, and the received wave was gained by 40 dB and attenuated by 11 dB. The bandwidth of the generated pulse was chosen to be 1 kHz-200 MHz to make the ultrasonic transducer as the bandwidth-limiting element of the system. After amplification, the received echoes from the specimens were displayed on a LeCroy WaveRunner 6200 oscilloscope with 0.1 ns timing resolution. ToF measurements were taken by measuring the difference in time of the peak amplitudes of the first two back-wall reflections and averaging over 500 transmitted pulses.

TABLE I. Parameters used in diffraction phase correction calculation.

Parameter	Value
Sound velocity, c	5.640 (mm/μs)
Distance traveled, $2Ln$ (n is echo #)	$22n$ (mm)
Transducer radius, a	3.175 (mm)
Frequency, f	9.00–10.00 (MHz)

After the phase and ToF measurements, the 10 MHz ultrasonic transducer was replaced with a 6.35 mm diameter, highly damped, broadband Olympus V214 ultrasonic transducer designed to operate at 50 MHz. Conventional pulse-echo ToF measurements were obtained with the transducer, similar to the measurements taken with the 10 MHz transducer.

C. Results and discussion

1. Correction for time-delay and phase offsets

Prior to analysis, the phase shift due to diffraction was found and subtracted out of the phase vs. frequency measurements. As borosilicate glass has no long-range crystal structure, it is assumed to be isotropic. Table I shows the parameters used to solve the diffraction correction integral at each frequency and for each echo. The nominal specimen thickness of $L = 11$ mm is used for each diffraction correction.

Figure 5 shows the computed diffraction phase correction curves for the first and second back-wall echoes and the phase difference between the same echoes. These curves were used to correct the measured phase vs. frequency response of the first and second back-wall echoes from each specimen. The diffraction phase correction provided an effect of −0.854 deg/MHz on the slope of the first echoes and −1.567 deg/MHz on the slope of the difference between back-wall echoes in the 9.00-10.00 MHz range, as shown in Fig. 5.

After diffraction correction, the effect of couplant reflection was removed by applying a linear fit to the ToF or phase vs. the measured thickness curve. The y-intercept of the line-of-best-fit at zero thickness corresponds to the extrapolated phase or time-delay offset. In total, 4 parameters were extracted

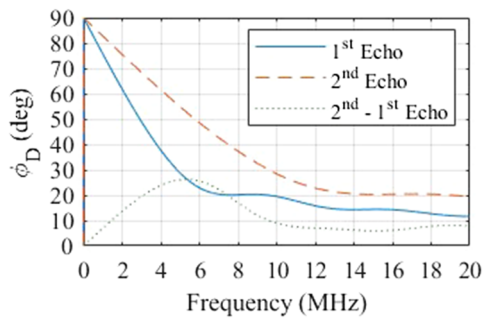

FIG. 5. Diffraction phase correction for 1st and 2nd back-wall echoes, as well as the phase difference between echoes.

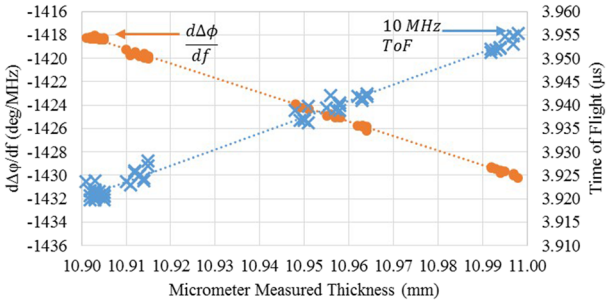

FIG. 6. Time delay parameter vs. thickness for each of the 54 locations, including the linear fit for the ToF with a 10 MHz transducer and $d\Delta\phi/df$ between consecutive back-wall echoes over the 9-10 MHz range.

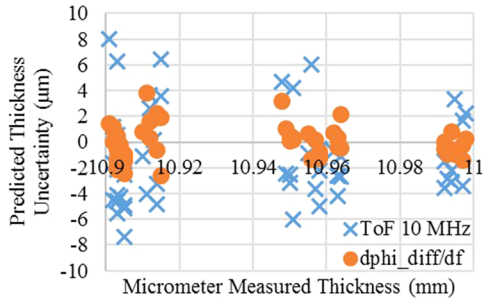

FIG. 7. Difference between the ultrasonically measured thickness and micrometer measured thickness for the ToF with a 10 MHz transducer and dΔϕ/df between consecutive back-wall echoes over the 9-10 MHz range.

from the ToF and phase measurements to predict the Borofloat glass thickness: ToF difference between echoes with a 10 MHz transducer, ToF difference between echoes with a 50 MHz transducer, slope of phase vs. frequency in the 9-10 MHz range from the first back-wall echo, and slope of the phase difference between back-wall echoes vs. frequency in the 9-10 MHz range.

Figure 6 shows plots of two of the time-delay parameters as a function of the specimen thickness. Included in each plot is the line-of-best-fit for the data, which is used to interpolate the time-delay or phase offset at zero specimen thickness. Assuming that the couplant thickness and quality are the same for each measurement, the offset measures the phase impact from all sources except for the test specimen. Comparing the phase difference between two consecutive echoes to the phase from the first echo, the phase offset dropped in magnitude, which is consistent with the theory that the phase difference would subtract out some external phase shift sources present in each echo.

As there is only a weak dependence of diffraction for the small ~100 μm thickness difference range, the diffraction corrections only provided a constant offset to the $d\phi/df$ vs. thickness measurement curves. As such, diffraction corrections did not provide a measureable effect on the thickness predictions in this experiment. It is noted, however, that the interpolation of the phase offset at zero thickness is only valid after diffraction corrections have been applied, according to Eqs. (4) and (5). By gaging thickness over a greater range, the diffraction correction to $d\phi/df$ will become more pronounced.

2. Glass thickness from ultrasonic measurements

After finding the phase or time-delay offset for each parameter, a thickness for each measurement was calculated from Eqs. (2) and (3). Figure 7 shows the difference between the ultrasonically measured thickness and micrometer measured thickness at each location, for two of the time-delay parameters. Additionally, Fig. 8 shows a box plot of the predicted thickness error from all of the parameters, displaying the median as well as the first and third quartiles of the data. Small plus signs in the box plot represent potential outlier data that fall outside of the quartiles by greater than 1.5 times the interquartile range. Note, *phi_diff* is the $\Delta\phi$ phase difference between the first and second back-wall echoes.

From comparing the predicted thicknesses with measurements with a calibrated micrometer, several conclusions can be drawn. The worst performing parameter tested was ToF measurements with the 10 MHz transducer, with the most significant mean and standard deviation of error. Using the same ultrasonic transducer, the CFPPLL-based ultrasonic measurement parameters performed more accurately and displayed less uncertainty. As predicted, the 50 MHz transducer performed more accurately and precisely than its 10 MHz counterpart. It is thought that the longer pulse duration from the 10 MHz transducer in comparison to the 50 MHz transducer results in higher uncertainty.

It is important to note that each of the CFPPLL-based phase parameters performed about the same or better in both accuracy and precision than the ToF measurements from the much higher frequency transducer. If the CFPPLL-based instrument was modified to have a pass-band around 50 MHz rather than 10 MHz, its thickness measurement resolution would be dropped by a factor of 5 since the phase resolution is constant with respect to the frequency. Thus, the CFPPLL-based method should outperform conventional ToF if operated at 50 MHz. In many media, attenuation coefficients are much larger at the higher frequencies; thus, a 50 MHz driving frequency may be impossible to use. Additionally, 50 MHz transducers are often very thin and easy to break, often requiring protective coverings or delay lines. As such, it is significant that the CFPPLL-based phase measurement method obtains similar thickness gaging performance at 10 MHz that conventional ToF measurements obtain at 50 MHz.

Additionally, the phase difference between consecutive echoes resulted in a decrease in the average error

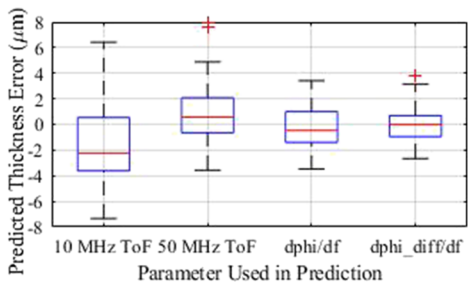

FIG. 8. Box plot of the predicted thickness error for each of the 4 time-delay or phase parameters.

and uncertainty for the $d\phi/df$ parameter. This provided the lowest mean error and uncertainty in the thickness of all parameters. $d\Delta\phi/df$ between the first and second back-wall echoes provided a mean predicted thickness error of −0.04 μm and standard deviation of predicted thickness error of 1.35 μm.

3. Phase measurement time

Measurements were recorded every 6 ms so that averaging over 256 measurements only took ~1.5 s. The measurement time can be further reduced by increasing the repetition rate of the transmitted sine wave train. The maximum repetition rate with this method depends on the ultrasonic attenuation in a given specimen so that echoes decay below the noise level prior to transmitting the next signal. In this specific setup, back-wall echo amplitudes dropped below the noise level after ~25 μs, meaning phase measurements averaged over 16 samples could be obtained in ~400 μs, making real-time high-resolution constant-frequency phase measurements possible, even with averaging to reduce uncertainty.

4. Internal sources of phase measurement uncertainty

Prior to investigating external sources of phase measurement uncertainty, the stability of phase measurements in the absence of changing transducer pressure and temperature was analyzed. The number of samples averaged for phase measurements within the microcontroller was changed in powers of four from $4^0 = 1$ to $4^4 = 256$. Figure 9 displays one standard deviation of phase measurements over a 30 min period with the temperature and transducer pressure held constant. The signal-to-noise ratio (SNR) for the first back-wall echo after narrowband filtering was measured to be 26.1 dB in this experiment. One least significant bit (LSB) of the phase shift within the DDS is 0.0220°. Thus, the standard deviation of phase due to the quantization error within the DDS is $LSB/\sqrt{12} = 0.0063°$, which is much lower than the phase errors shown in Fig. 9. As such, white noise appears to contribute much more to the phase error than ADC quantization noise. It is thought that better suppression of the transmitted wave during the receiving period of the circuit and more narrowband filtering may help improve the SNR.

As shown in Fig. 9, averaging over as few as 16 samples has a large effect on the phase measurement error, bringing the uncertainty below the phase adjustment resolution of the DDS of 0.022°. Averaging over more samples continues to drop the phase measurement uncertainty to below 0.01° at 256 samples. The CFPPLL-based method outperforms high resolution cross-correlation ToF methods because of the phase error due to white noise and quantization error. As the effects of changing environmental factors were removed in this experiment, the phase measurement uncertainty over a long period of time should only be due to the ADC quantization error and random noise. Thus, it should be comparable to the phase error in cross-correlation methods due to the quantization error and white noise. By comparing Fig. 9 in this work with Fig. 2 of Ref. 19 by Liang *et al.*, the improvement in phase error for smaller SNRs can be seen. In this work, the measured SNR of 26.1 dB and 14 bit ADC produced a standard deviation of phase error of under 0.02° with 16 samples, while the cross-correlation method in Ref. 19 requires much higher SNRs or samples averaged to obtain similar phase errors. Using the same SNR of 26.1 and assuming that the phase error due to white noise and quantization error are approximately equal, the standard deviation of phase error with 256 samples for cross correlation is 0.251° according to Eq. (22) in Ref. 19, compared to 0.008° measured with the CFPPLL-based method.

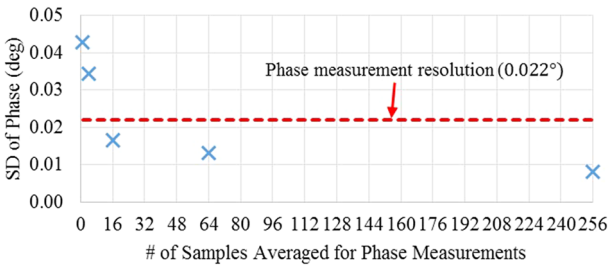

FIG. 9. Standard deviation of phase over 30 min period vs. number of samples averaged for phase measurements.

5. External sources of phase measurement uncertainty

To improve the accuracy of phase measurements, the external sources of uncertainty have also been analyzed. Measurements of pressure applied to the transducer and ambient temperature during testing allowed for the impact of these sources of uncertainty to be examined. From an experiment tracking the phase shift due to pressure on the ultrasonic transducer, the phase was found to level off around ~2 MPa, above which $\partial\phi/\partial f$ varied linearly by 0.439 (deg/MHz)/MPa and the phase at 10 MHz varied by 3.915° MPa^{-1}. During thickness gaging experiments, the mean pressure on the transducer was measured to be 2.754 MPa with a standard deviation of 0.031 MPa. Therefore, the phase measurement uncertainty due to applied pressure differences is 0.014° MHz^{-1} for $d\phi/df$ and 0.112° for the phase at 10 MHz.

The phase shift at 10 MHz in the glass specimens due to small temperature variations was found to vary linearly 0.715 deg/°C in the 20 °C-25 °C range, based on testing in an environmental chamber. The mean temperature during ultrasonic thickness gaging tests was measured to be 20.51 °C with a standard deviation of 0.18 °C. Using the relationship between the phase and temperature found in an environmental chamber experiment, the phase measurement uncertainty at 10 MHz due to temperature uncertainty is 0.129°.

The standard deviation in phase measurements at 10 MHz due to external sources is 0.171°, which is combined with the measured internal phase measurement uncertainty at 10 MHz, while averaging over 16 samples of 0.017° to yield a total phase uncertainty at 10 MHz of 0.172°. Conversion to thickness measurement uncertainty in the Borofloat glass via Eq. (1) gives a standard deviation of thickness measurement uncertainty of 0.14 μm due to transducer pressure and temperature variations. Combined with the measurement uncertainty of the calibrated micrometer in the 10.9-11.0 mm thickness range, the thickness measurement uncertainty due to the micrometer

uncertainty, temperature variations, and transducer pressure variations is 1.06 μm. Thus, most of the 1.35 μm uncertainty using the $d\Delta\phi/df$ phase measurement method is attributed to known sources, the bulk of which is from the micrometer thickness measurements. Comparing the CFPPLL-based ultrasonic phase measurements with a more accurate method or using test specimens with thicknesses known to submicron tolerances should improve the predicted thickness uncertainty.

Another potential source of uncertainty is the slight nonlinearity of the phase response in the 9-10 MHz range introduced by the reflection off of the couplant layer. Using the slope of the phase vs. frequency response of back-wall reflections depends on the linear relationship between the phase and frequency of the test specimen, as described by Eq. (1). However, the reflection from the thin couplant layer has an upward concavity, as seen in Fig. 4, and can only be approximated as linear over a sufficiently small frequency range. Consequently, measurement accuracy and uncertainty could be further improved by sweeping over a smaller frequency range.

A final source of uncertainty is inconsistent flatness and parallelism of the test specimens. As seen in the thickness values from Fig. 6, the specimens varied in thickness across their surfaces as much as 14 μm. Thus, the glass specimens do have some inherent lack of flatness or parallelism which contributes to the uncertainties observed. No attempt to correct the phase measurements for flatness and parallelism issues was conducted in this work.

IV. CONCLUSIONS

A novel single-frequency ultrasonic phase measurement instrument has been built and tested to show its efficacy against conventional ultrasonic time-delay measurement methods. The instrument is digitally controlled and based on a CFPPLL design, which allows an unprecedented frequency independent ultrasonic phase measurement resolution of 0.000 38 rad (0.022°) or one part in 6.1×10^{-5} of an ultrasonic wavelength. The ultrasonic phase can be tracked in real-time for the measurement of material property changes due to external stimuli. Unlike previous PPLL-based ultrasonic phase measurement instruments, the system can change driving frequency while also maintaining the previous phase relationship, so swept-frequency phase measurements can be conducted with resolution as low as 3.55 μHz. This new feature allows absolute sound velocity or thickness measurements to be obtained in solid media, opening up this instrument to many new applications beyond simple phase or sound velocity monitoring, like previous ultrasonic PPLL instruments.

Using glass specimens, swept-frequency ultrasonic phase measurements from the CFPPLL instrument were compared with conventional, broadband ToF measurements from a pulser-receiver. After correcting for diffraction effects and factoring out the time-delay offset due to external sources, the CFPPLL phase measurements outperformed conventional ToF measurements in both accuracy and precision. Furthermore, CFPPLL phase measurements near 10 MHz outperformed much higher frequency 50 MHz ToF measurements. The slope of the phase vs. frequency line taken with the CFPPLL instrument was able to predict the thickness with an average error of −0.04 μm and standard deviation of error of 1.35 μm, which was close to the calibrated micrometer's 1.06 μm uncertainty. Given a nominal thickness of 10.95 mm, the mean thickness measurement error was −0.000 37% of the total thickness and the standard deviation of thickness measurement uncertainty was 0.012%. Additional studies showed that the CFPPLL method produces a standard deviation of phase error of only 0.008° due to the quantization error and system noise, in comparison to a phase error of 0.251° for high-resolution cross-correlation phase measurements using the same SNR as 26.1 dB and number of samples as 256.

The newly developed, digitally controlled CFPPLL-based phase measurement instrument can provide high-resolution, low-uncertainty ultrasonic time-delay measurements. Its digital control and waveform generation provide major improvements in both resolution and ease-of-use to previous PPLL-based ultrasonic phase measurement instruments. The additional ability to conduct swept-frequency absolute phase measurements will have applications of a wide variety of new areas. In addition to improving on conventional ToF methods of sound velocity or thickness measurements in solids or liquids, high-resolution swept-frequency phase measurements may have applicability in areas such as adhesive bond quality assessment, thin film characterization, and ultrasonic analysis of complex structures, such as composites.

ACKNOWLEDGMENTS

The authors would like to thank Angela Selden and John Callahan for their work in building and testing parts of the CFPPLL instrument. This work was supported by a NASA Space Technology Research Fellowship and the NASA Langley Professor Program.

[1]H. J. McSkimin, J. Acoust. Soc. Am. **33**, 12 (1961).
[2]E. P. Papadakis, J. Acoust. Soc. Am. **42**, 1045 (1967).
[3]R. Odru, C. Riou, J. Vacher, P. Deterre, P. Peguin, and F. Vanoni, Rev. Sci. Instrum. **49**, 238 (1978).
[4]S. Taki, Y. Furuta, and T. Takamura, Rev. Sci. Instrum. **52**, 1388 (1981).
[5]G. Horvath-Szabo, M. Hoiland, and E. Hogseth, Rev. Sci. Instrum. **65**, 1644 (1994).
[6]D. J. McClements and P. Fairley, Ultrasonics **29**, 58 (1991).
[7]T. Pialucha and P. Cawley, Ultrasonics **32**, 431 (1994).
[8]A. I. Lavrentyev and S. I. Rokhlin, J. Acoust. Soc. Am. **102**, 3467 (1997).
[9]C. Jin, Rev. Sci. Instrum. **67**, 271 (1996).
[10]U. Kaatze, F. Eggers, and K. Lautscham, Meas. Sci. Technol. **19**, 062001 (2008).
[11]D. Marioli, C. Narduzzi, C. Offelli, D. Petri, E. Sardini, and A. Taroni, IEEE Trans. Instrum. Meas. **41**, 93 (1992).
[12]D. R. Hull, H. E. Kautz, and A. Vary, in Spring Conference of the American Society for Nondestructive, 1984.
[13]J. D. Aussel and J. P. Monchalin, Ultrasonics **27**, 165 (1989).
[14]I. Fujii and K. Kawashima, Rev. Prog. Quant. Nondestr. Eval. **14**, 203 (1995).
[15]R. E. Guerjouma, A. Mouchtachi, Y. Jayet, and J. C. Baboux, in *IEEE International Ultrasonics Symposium* (IEEE, 1992).
[16]P. Brassier, B. Hosten, and F. Vulovic, Flow Meas. Instrum. **12**, 201 (2001).
[17]S. Hirata, M. K. Kurosaw, and T. Katagiri, Acoust. Sci. Technol. **30**, 429 (2009).
[18]T. Chen, P. Que, O. Zhang, and Q. Liu, Russ. J. Nondestr. Test. **41**, 594 (2005).
[19]Y.-R. Liang, H.-Z. Duan, H.-C. Yeh, and J. Luo, Rev. Sci. Instrum. **83**, 095110 (2012).
[20]R. J. Blume, Rev. Sci. Instrum. **34**, 1400 (1963).

[21]J. S. Heyman and E. J. Chern, J. Test. Eval. **10**, 202 (1982).
[22]W. T. Yost, J. H. Cantrell, and P. W. Kushnick, J. Acoust. Soc. Am. **91**, 1456 (1992).
[23]W. T. Yost, J. H. Cantrell, and P. W. Kushnick, Rev. Sci. Instrum. **62**, 2451 (1991).
[24]K.-Y. Jhang, H.-H. Quan, J. Ha, and N.-Y. Kim, Ultrasonics **44**, e1339 (2006).
[25]S. Adenwalla, S. W. Lin, Q. Z. Ran, Z. Zhao, J. B. Ketterson, J. A. Sauls, L. Taillefer, D. G. Hinks, M. Levy, and B. K. Sarma, Phys. Rev. Lett. **65**, 2298 (1990).
[26]P. Palanichamy, A. Joseph, T. Jayakumar, and B. Raj, NDT&E Int. **28**, 179 (1995).
[27]P. H. Nicholson, G. Lowet, C. M. Langton, J. Dequeker, and G. Van der Perre, Phys. Med. Biol. **41**, 2421 (1996).
[28]M. Cutroni and A. Mandanici, J. Chem. Phys. **114**, 7124 (2001).
[29]T. Ueno, B. R. Macias, W. T. Yost, and A. R. Hargens, J. Neurosurg. **103**, 361 (2005).
[30]V. N. Bindal, J. Sci. Ind. Res. **59**, 935 (2000).
[31]M. Redwood and J. Lamb, Proc. Inst. Electr. Eng., Part B **103**, 773 (1956).
[32]T. Inamura, Jpn. J. Appl. Phys., Part 1 **9**, 255 (1970).
[33]Y. H. Kim, S. J. Song, J. K. Lee, S. S. Hong, and H. S. Eom, J. Korean Soc. NDT **22**, 621 (2002).
[34]A. Vincent, Ultrasonics **25**, 237 (1987).
[35]J. Williams and J. Lamb, J. Acoust. Soc. Am. **30**, 308 (1958).
[36]T. Reddyhoff, S. Kasolang, R. S. Dwyer-Joyce, and B. W. Drinkwater, Proc. Inst. Mech. Eng., Part J **219**, 387 (2005).
[37]H. B. Huntington, A. G. Emslie, and V. W. Hughes, J. Franklin Inst. **245**, 1 (1948).
[38]H. Seki, A. Granato, and R. Truell, J. Acoust. Soc. Am. **28**, 230 (1956).
[39]A. O. Williams, J. Acoust. Soc. Am. **23**, 1 (1951).
[40]E. Papadakis, J. Acoust. Soc. Am. **40**, 863 (1966).
[41]A. S. Khimunin, Acoustica **39**, 87 (1978).
[42]J. Kushibiki and M. Arakawa, J. Acoust. Soc. Am. **108**, 564 (2000).
[43]K. Negishi, K. Takgi, and H. Ozawa, J. Acoust. Soc. Jpn. **1**, 11 (1980).
[44]P. H. Rogers and A. L. Van Buren, J. Acoust. Soc. Am. **55**, 724 (1974).